FLIGHT RESEARCH DIVISION

OFFICE MEMO

Capt C. D. Zaleski

December 1964

AV-64-8

NF-104A LATERAL-DIRECTIONAL STABILITY ANALYSIS

Part of the NF-104A flight test program was to investigate the lateral-directional stability at high Mach numbers with the speed brakes extended. This flight condition was encountered during the entry following a zoom mission and no previous data were available. The data available for the speed brakes retracted configuration indicated that the directional stability parameter, C_{n_β} decreased with increasing Mach number, and it was also known that the speed brakes detracted from the stability. The study received impetus when a lateral-directional oscillation was encountered on several NF-104 flights during the recovery from the high altitude portion of the zoom mission. In each case where these oscillations were encountered, the following conditions existed.

1. High Mach number
2. Angle of attack greater than 5 degrees
3. Jet engine shut down
4. Rocket engine off
5. Stability augmentation on
6. Speed brakes extended
7. Reaction control system (RCS) damper inactive

The pilot was able to damp these oscillations by lowering his angle of attack. (Figure 1). On flights 5 and 8 of the flight test program, the oscillations built up almost immediately after the RCS dampers were switched off. On flight 10, the oscillations occured during a period of no RCS inputs, and they were damped out when the RCS damper inputs came on.

TEST METHOD

In order to study the lateral-directional characteristics of the NF-104 at these zoom recovery conditions, a low, flat zoom trajectory was devised using the NF-104 three degree of freedom simulation. (Reference 1). This mission enabled the duplication of the Mach number, angle of attack, and dynamic pressure of a zoom recovery, but did not require the high angle of attack for a safe recovery. Thus, lowering the angle of attack was a safe means of getting out of trouble at any time during the lateral-directional investigations.

The technique used to get the stability data was to light the rocket at Mach 2 and pull up to a pitch attitude of 25°. At an altitude of 65,000 ft, the pilot pushed over to zero "g" and came level about 80,000 ft and Mach 2. The rocket engine and jet engine were then shut down, the speed brakes extended, and the aircraft stabilized at the desired angle of attack. The pilot then turned off the roll and yaw stability augmentation and performed a rudder pulse at constant angle of attack wile making a minimum of aileron inputs. Because of the rapid deceleration, in order to get the high Mach number data point, it was necessary to leave the engines on until after the angle of attack was stabilized, the speed brakes extended, and the dampers turned off. In Table I, the Mach number, angle of attack, dynamic pressure, weight, and center of gravity of the test points have been summarized. The Mach numbers ranged from 1.3 to 2.1 and angle of attack from 4 degrees to 13 degrees.

METHOD OF ANALYSIS

The object of the analysis was to determine the stability derivatives C_{n_β} and C_{l_β}. The analog matching technique was the primary method of analysis. This method entailed the use of an analog computer simulation of NF-104 lateral-directional aerodynamics. The procedure was to duplicate on the simulator the flight conditions and aircraft weight and center of gravity at each data point and introduce into the computer the same control surface inputs which occurred in flight. The stability derivatives,

primarily C_{n_β} and C_{l_β}, were then varied until the time history of the computer response in roll rate, roll angle, sideslip angle, and yaw rate matched as closely as possible the history of the aircraft response which had been recorded by an oscillograph. When the responses closely matched, the values of C_{n_β} and C_{l_β} which had been required by the simulation were recorded as the results of the analysis. This method of analysis is valid regardless of control inputs by the pilot, since they can be introduced into the simulation and taken into account. Thus it was possible to obtain results from the oscillations encountered on the earlier high zoom recoveries despite large control inputs by the pilot during the maneuver. In Reference 2, the analog matching technique has been described in more detail.

A secondary method of analysis was to use the natural frequency of the oscillations and the best known value of C_{l_β} to calculate C_{n_β} from the following body axis equations for the lateral-directional stability parameter ($C_{n_\beta}^*$): (Appendix I)

$$C_{n_\beta}^* = \frac{\omega_n^2 I_z}{qSb\ (57.3)} \simeq C_{n_\beta} \cos\alpha - \frac{I_{xz}}{I_x} C_{l_\beta} \sin\alpha$$

$$+ \frac{I_{xz}}{I_x} [C_{l_\beta} \cos\alpha - C_{n_\beta} \sin\alpha]$$

The analog matching results were checked by substituting C_{n_β} and C_{l_β} into the equation for $C_{n_\beta}^*$ and comparing with the value of $C_{n_\beta}^*$ obtained using the natural frequency ω_n (rad/sec) obtained from the flight data. Figure 2 shows the comparison of results. The value of $C_{n_\beta}^*$ had a range of values in some cases because the period of the oscillations varied slightly during the maneuver.

ASSUMPTIONS

The equations used in the analog matching were the lateral-directional equations of motion of a rigid airplane with linearized stability derivatives assumed (Appendix I). Consequently, angle of attack was assumed

to be constant and pitch rate to be zero. In addition, dynamic pressure was assumed to be constant for each maneuver. Angle of attack generally stayed within $\pm$ 1/2 degree of the average value used in the calculations, and dynamic pressure was $\pm$ 10% of its average value.

In the equation used to calculate C_{n_β} from the natural frequency and a known C_{l_β}, all the side force terms, the damping derivatives, and the control derivatives were neglected in addition to the assumptions made for analog matching.

DISCUSSION OF RESULTS

The results of the analysis are presented in Figures 5 through 10 showing C_{n_β} corrected to center of gravity of 21% and 25% and C_{n_β} and C_{l_β} in both body axes and stability axes. This is done for convenience in making comparisons. The NF-104 stability axes wind tunnel data are also presented in Figure 11. (Reference 4).

The effect of the speed brakes was to lower the level of C_{n_β} (Figure 5) and C_{l_β} (Figures 8 and 10). Mach number had only a slight effect on C_{l_β} (Figure 6 and 8), but C_{n_β} decreased with Mach number in both speed brake configurations. It should be emphasized that C_{n_β} continued to decrease as Mach number increased above Mach 2.0 although not as rapidly as at the lower Mach numbers.

Insufficient data were obtained and scatter was too great to quantitatively define the effect of angle of attack on C_{n_β} and C_{l_β}. It may be noted from any of the C_{n_β} plots that between Mach 1.6 and 1.8 there are several points above the faired curve. These points are high angle of attack points, and it can be stated that in this Mach region C_{n_β} increases with angle of attack at least until $\alpha = 13°$. The effect of angle of attack explains the scatter of the brakes extended points on Figure 2. The two curves on this plot were calculated from the single curves of C_{n_β} and C_{l_β} on Figure 6 using two different angles of attack in order to show the effect of angle of attack on the lateral-directional stability parameter $C_{n_\beta}^*$.

There were several data points for which the phase of yaw rate and roll rate could not be matched simultaneously. The cause of this was not determined and was attributed to either instrumentation errors or aircraft flexibility effects. Although the phase matching problem existed, it was felt that in each case the analog match obtained was valid, because as C_{n_β} and C_{l_β} were varied from the chosen values, the match became progressively worse. The closeness with which the calculated values agreed with the values obtained by analog matching also tended to verify the analog matching values. (Figure 2).

A significant discrepency between the analog response and some of the flight test data was found. When compared with the analog response to the same control surface inputs, the aircraft response seemed to be excited by an additional forcing function which caused the oscillations to diverge to a limit cycle amplitude. This divergence could not be duplicated with the analog simulation even though the phase and frequency could be matched, and any constant amplitude could be obtained by varying either rudder effectiveness or the initial conditions on the sideslip angle, roll rate and yaw rate. It was concluded during the program that both the lateral-directional oscillations encountered during zoom recoveries and the limit cycles encountered following rudder pulses during the test program were caused by an external forcing function which was not accounted for by the normal NF-104 aerodynamics as represented in the analog simulation. During flight 34, the last stability flight, the jet engine was allowed to run during the rudder pulse at Mach 2.12. After about two cycles of a damped oscillation, the jet engine was shut down. Immediately the oscillations diverged to approximately $\pm 5°$ of sideslip. The oscillation damped out gradually as angle of attack was lowered and Mach number bled off. (Figure 3A and 3B). It was then concluded that the forcing function which caused the divergence was an oscillatory duct spillage condition that occurred at certain angles of attack and Mach numbers when the engine was off. An approximate boundary for these oscillations in terms of angle of attack and Mach number has been given in Figure 4. The F-104 aircraft had an earlier history of oscillations induced by unstable inlet duct conditions. The duct splitter was installed as a solution to a problem which arose as a result of divergent lateral-directional oscillations following compressor stalls. (Reference 3).

Aside from the duct spillage problem, the results of the lateral-directional stability analysis indicated that the levels of static stability, C_{n_β} and C_{l_β}, were sufficient to provide satisfactory handling qualities up to at least Mach 2.12 (the highest Mach number tested) under the conditions which normally existed during a zoom recovery (listed on page 1). A "worst fairing" of brakes extended data showed that C_{n_β} could go to zero at Mach 2.3 (Figure 6). However, total static lateral-directional stability, as indicated by the parameter $C_{n_\beta}^*$, appeared to be positive to at least Mach 2.3 (Figure 2). The dynamic instability, apparently due to duct spillage at high Mach numbers and angles of attack, indicated restriction of the practical use of the aircraft with the jet engine shut down to below approximately Mach 2.0. (Figure 4).

CONCLUSIONS

Values for the stability derivatives C_{n_β} (yawing moment due to sideslip) and C_{l_β} (rolling moment due to sideslip) were determined from flight test data for the NF-104 between Mach 1.3 and 2.1 with the speed brakes retracted and extended.

At Mach numbers above 1.6 and high angles of attack with the jet engine shut down, the lateral-directional mode of the aircraft was excited by engine air inlet duct spillage. This duct spillage condition was oscillatory and caused the oscillations of the aircraft to diverge to a limit cycle amplitude at some flight test conditions. (Figure 4).

Although the static lateral-directional stability appeared to be satisfactory even above Mach 2.12, the dynamic instability due to duct spillage indicated restriction of the practical use of the aircraft to below approximately Mach 2.0 with the jet engine shut down.

REFERENCES

1. Zaleski, Charles D, and Landry, Lloyd M., "NF-104A Analog Simulation Support," Flight Research Division Office Memo, December 1964.

2. Rampy, Johnny M., and Berry, Donald T., "Determination of Stability Derivatives from Flight Test Data by Means of High Speed Repetitive Operation Analog Matching," AFFTC TDR 64-8, May 1964.

3. Hoey, Robert G., and Kincheloe, Ivan C., "F-104A Stability and Control," AFFTC TR 58-14, April 1958.

4. "Aerospace Trainer Stability Verification Test in LFL 4' x 4' Supersonic Wind Tunnel," Data Release, LFL 5-39, 6-6-62.

TABLE I

FLIGHT #	PULSE #	MACH #	ANGLE ATTACK DEG	DYNAMIC PRESSURE lbs/ft^2	WEIGHT lbs	c.g. % mac	DRAG BRAKES EXTENDED OR RETRACTED
5		1.87	7.7	325-425	15,500	16.5	ext
8		1.78	8	320	15,667	18.0	ext
10		1.93	5.25	522	15,037	18.6	ext
16	1	1.93	4.5	170	15,980	14.0	ret
	2	1.88	8.4	199			ret
	3	1.79	8.0	241.8			ret
	4	1.67	10.0	242.2			ret
	5	1.46	10.2	188.8			ext
17	1	1.89	9.8	184	15,980	14.0	ret
	2	1.75	9.6	188			ext
	3	1.56	5.8	190			ext
18	1	1.81	7.0	160.2	15,800	14.2	ext
23	1	1.78	10.9	144	16,262	15.0	ext
	2	1.69	6.1	142			ext
	3	1.64	10.0	174			ext
	4	1.48	11.1	180			ext
	5	1.33	5.4	160			ext
24	1	1.70	10.6	116.5	15,835	16.3	ext
	2	1.63	12.0	119			ext
31	1	1.77	10.5	213	15,538	16.8	ext
34	1	2.12	8.2	257	16.103	13.5	ext

Representative Moments of Inertia

$I_x = 4240$

$I_{xz} = 4500$

$I_z = 75,000$

APPENDIX I

Summary of Equations

1. Equations used in Lateral-Directional Analog Matching:

$$I_x \dot{P} = I_{xz} \dot{R} + qSb \left[C_{l_\beta} \beta + C_{l_{\delta_r}} \delta_r + C_{l_{\delta_a}} \delta_a + C_{l_R} \frac{Rb}{2V} + C_{l_p} \frac{Pb}{2V}\right]$$

$$\dot{\beta} = P \sin \alpha - R \cos \alpha + \phi \frac{g}{V} \cos \alpha + qSb \left[C_{y_\beta} \beta + C_{y_{\delta_r}} \delta_r + C_{y_{\delta_a}} \delta_a\right]$$

$$I_z \dot{R} = I_{xz} \dot{P} + qSb \left[C_{n_\beta} \beta + C_{n_{\delta_r}} \delta_r + C_{n_{\delta_a}} \delta_a + C_{n_p} \frac{Pb}{2V} + C_{n_R} \frac{Rb}{2V}\right]$$

2. Assumptions used in matching:

$$\sin \phi \approx \phi \; ; \; \beta \approx \frac{v}{V} \; ; \; \dot{\beta} = \frac{\dot{v}}{V}$$

3. Equations used to derive analytical expression for $C_{n_\beta}^*$:

$$C_{n_\beta}^* = \frac{\omega_n^2 I_z}{(57.3)\ qSb} = C_{n_\beta} \cos \alpha - \frac{I_z}{I_x} C_{l_\beta} \sin \alpha + \frac{I_{xz}}{I_x} \left[C_{l_\beta} \cos \alpha - C_{n_\beta} \sin \alpha\right]$$

$$I_x \dot{P} = I_{xz} \dot{R} + qSb\, C_{l_\beta}$$

$$\dot{\beta} = P \sin \alpha - R \cos \alpha$$

$$I_z \dot{R} = I_{xz} \dot{P} + qSb\, C_{n_\beta} \beta$$

4. Additional assumptions for $C_{n_\beta}^*$ equation:

$$\delta_a = \delta_r = 0$$

$$C_{l_p} = C_{l_R} = C_{n_p} = C_{n_R} = 0$$

$$C_{y_\beta} = C_{y_{\delta_r}} = C_{y_{\delta_a}} = \phi = 0$$

5. Equation used for center of gravity correction:

$$C_{n_{\beta(.25c)}} = C_{n_{\beta_{(c.g.)}}} + C_{y_\beta} \frac{c}{b} (.25\ c - c.g.)$$

Each point was corrected for c.g., and the curves were corrected by using average c.g. = .152 c.

6. Transformation between body axes and stability axes:

$$C_{n_{\beta_s}} = C_{n_{\beta_B}} \cos \alpha - C_{l_{\beta_B}} \sin \alpha$$

$$C_{l_{\beta_s}} = C_{l_{\beta_B}} \cos \alpha + C_{n_{\beta_B}} \sin \alpha$$

Each point was converted separately using the appropriate α. The curves were converted using average $\alpha = 8°$.

LIST OF SYMBOLS

Symbol	Definition	Units
p	roll rate	rad/sec
Q	pitch rate	rad/sec
R	yaw rate	rad/sec
$I_{x,y,z}$	moment of inertia about body x, y, z axis	slug ft^2
I_{xz}	product of inertia	slug ft^2
α	angle of attack	degrees
β	sideslip angle	radians/degrees
ϕ	bank angle	radians
u	velocity along body x axis	ft/sec
v	velocity along body y axis	ft/sec
q	dynamic pressure	lbs/ft^2
S	wing area (F104A Ref)	196.1 ft^2
b	wing span (F104A Ref)	21.9 ft^2
c	mean aerodynamic chord	9.55 ft
δ_a	aileron position	degrees
δ_r	rudder position	degrees
$C_{n_\beta}^*$	lateral-directional stability parameter	per degree
C_{n_β}	yawing moment coefficient derivative	per degree
C_{l_β}	rolling moment coefficient derivative	per degree
C_{l_p}, C_{n_R}, C_{l_R}, C_{n_p}	damping derivatives	per radian
$C_{n_{\delta_r}}$, $C_{l_{\delta_a}}$, $C_{n_{\delta_a}}$, $C_{l_{\delta_r}}$, $C_{y_{\delta_r}}$, $C_{y_{\delta_a}}$	control derivatives	per degree
C_{y_β}	side force derivative	per degree
ω_n	natural frequency	rad/sec
g	acceleration of gravity	ft/sec^2

ANGLE OF ATTACK AND MACH NUMBER AT WHICH OSCILLATIONS OCCURRED DURING NF104A ZOOM RECOVERIES

13 NOV 64

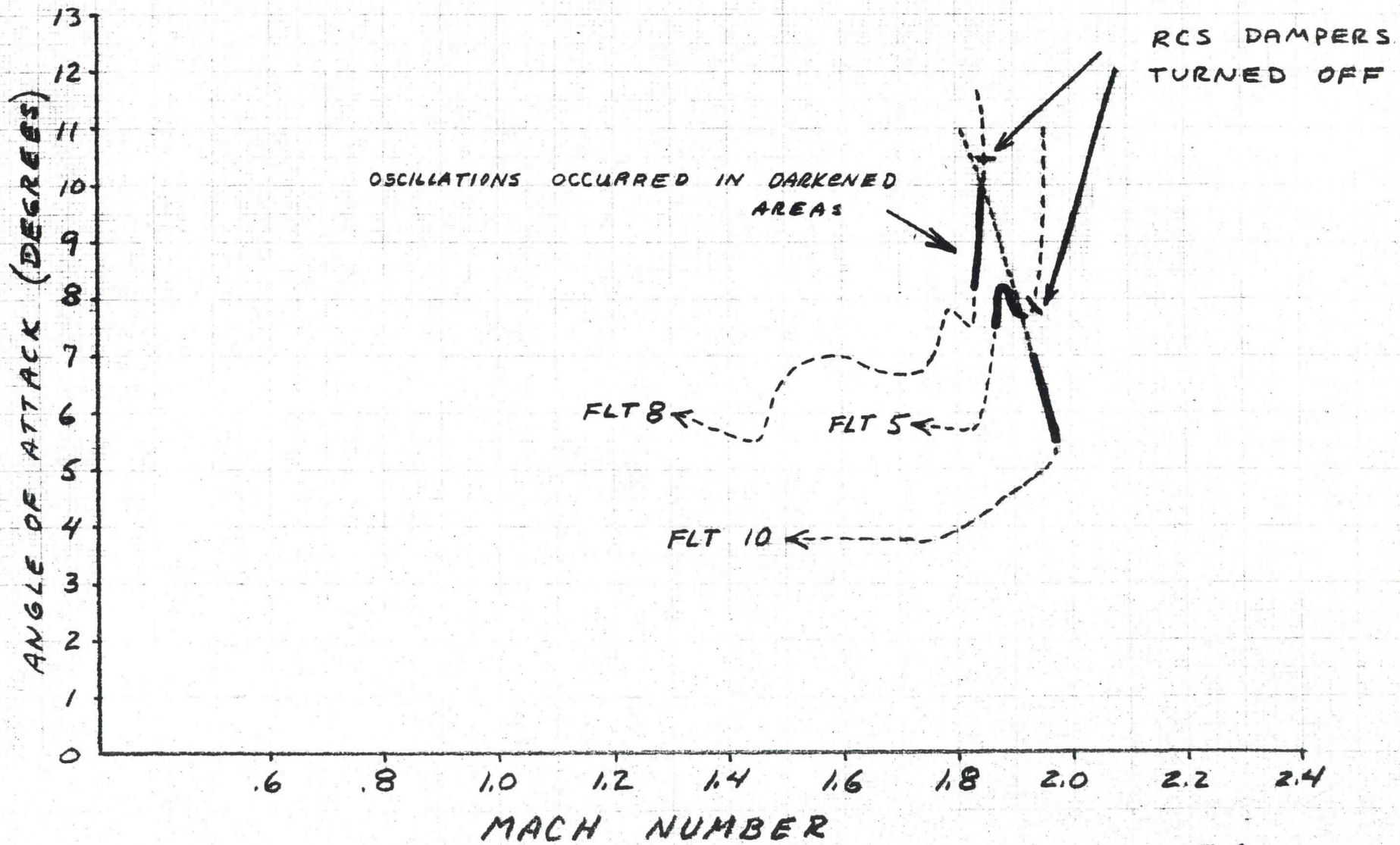

FIG 1

COMPARISON OF ANALOG MATCHING RESULTS
WITH
CALCULATIONS OF THE LATERAL-DIRECTIONAL STABILITY
PARAMETER, $C_{m_\beta}^*$, MADE DIRECTLY FROM FLIGHT TEST RESULTS

13 NOV 64

+ — $C_{m_\beta}^* = \dfrac{\omega_n^2 I_z}{(57.3)\, q S b}$ CALCULATED FROM FLIGHT TEST DATA

+ ⋮ + } RANGE

▽ — $C_{m_\beta}^* = C_{m_\beta} \cos\alpha - \dfrac{I_z}{I_x} C_{l_\beta} \sin\alpha + \dfrac{I_{xz}}{I_x}\left[C_{l_\beta}\cos\alpha - C_{m_\beta}\sin\alpha\right]$ { CALCULATED FROM BODY AXES C_{m_β} + C_{l_β} OBTAINED FROM ANALOG MATCHING

▼ — SPEED BRAKES RETRACTED

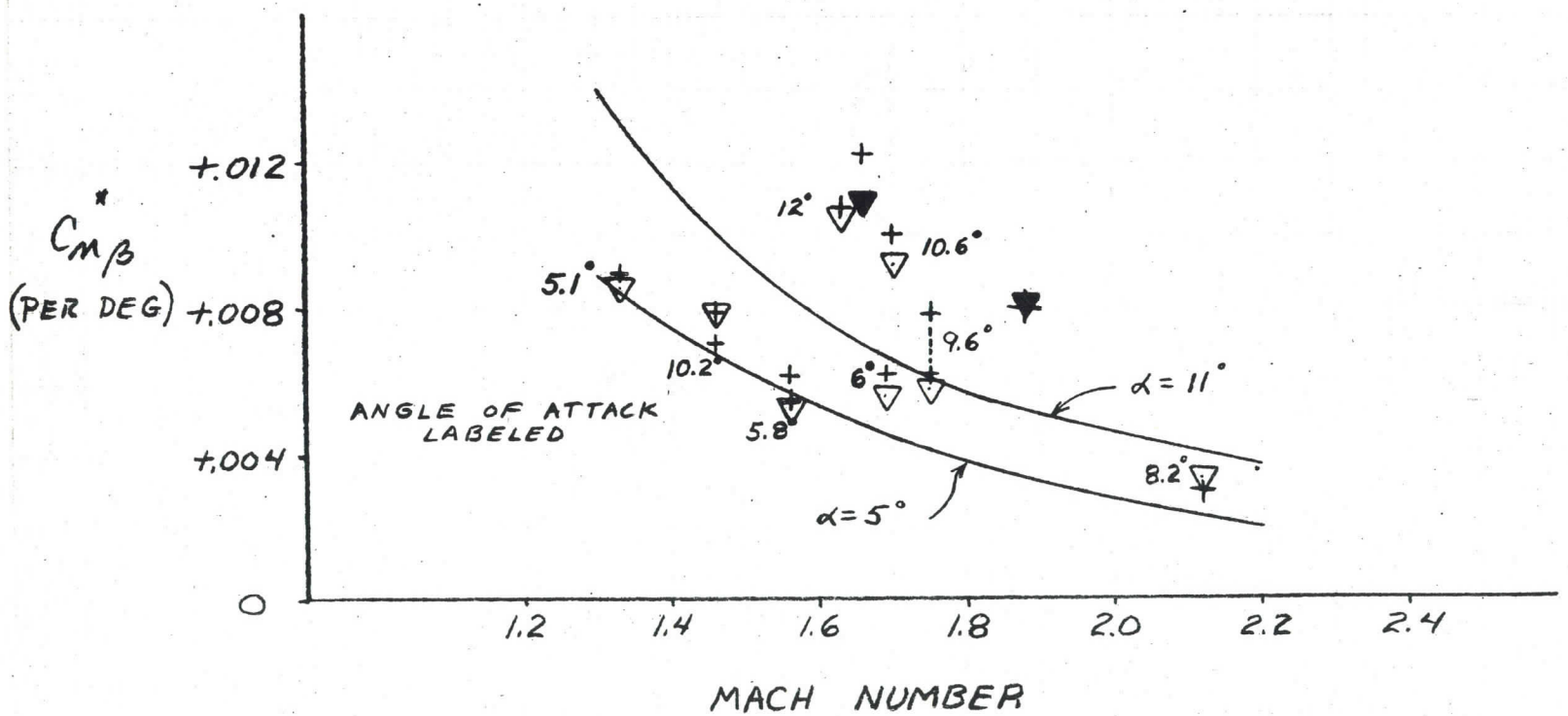

FIG 2

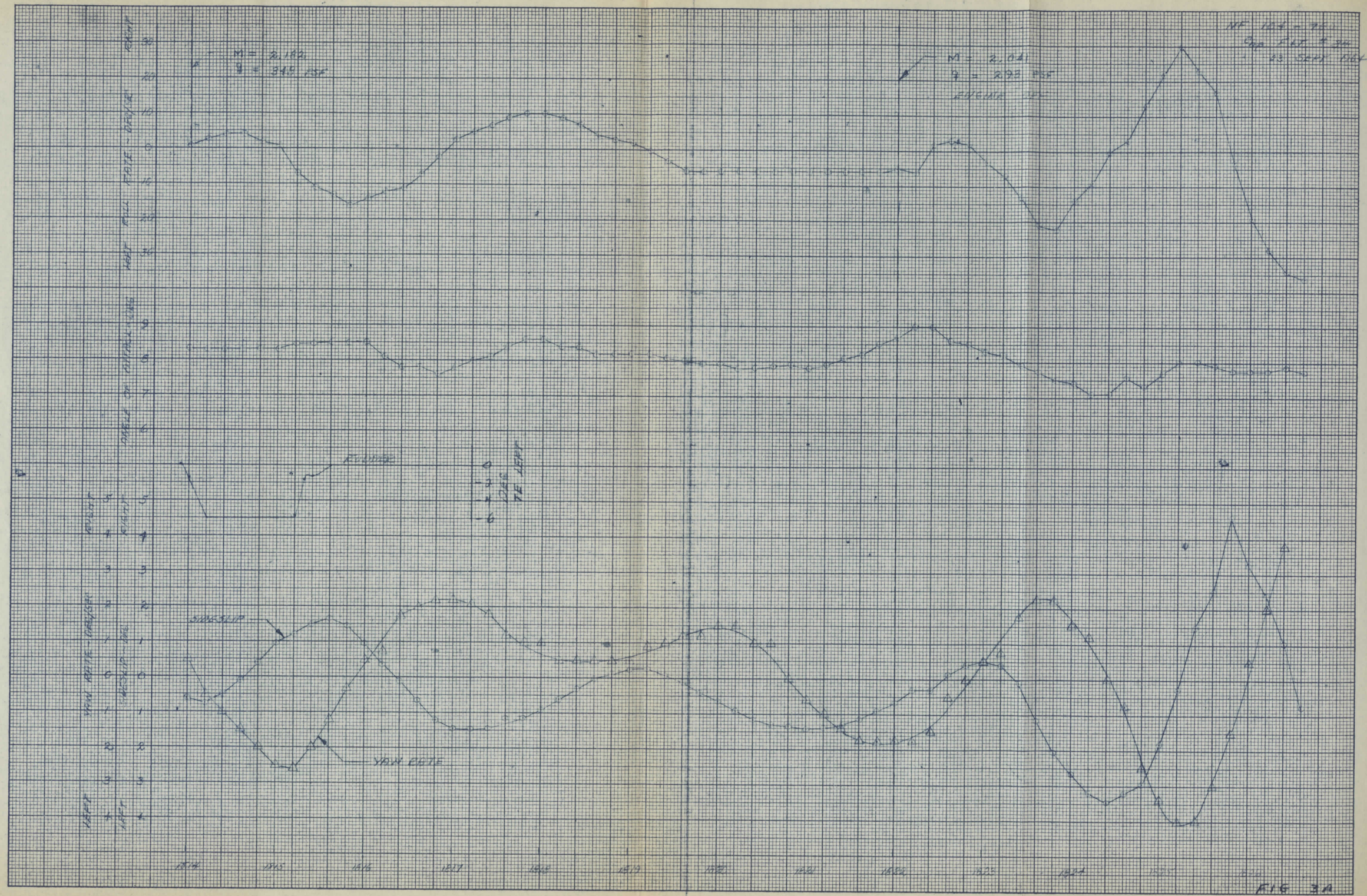

FIG 3A

K+E KEUFFEL & ESSER CO. MADE IN U.S.A. 359-1-T5 10 X 10 TO THE CM. ENGINEERING LITHOGRAPH

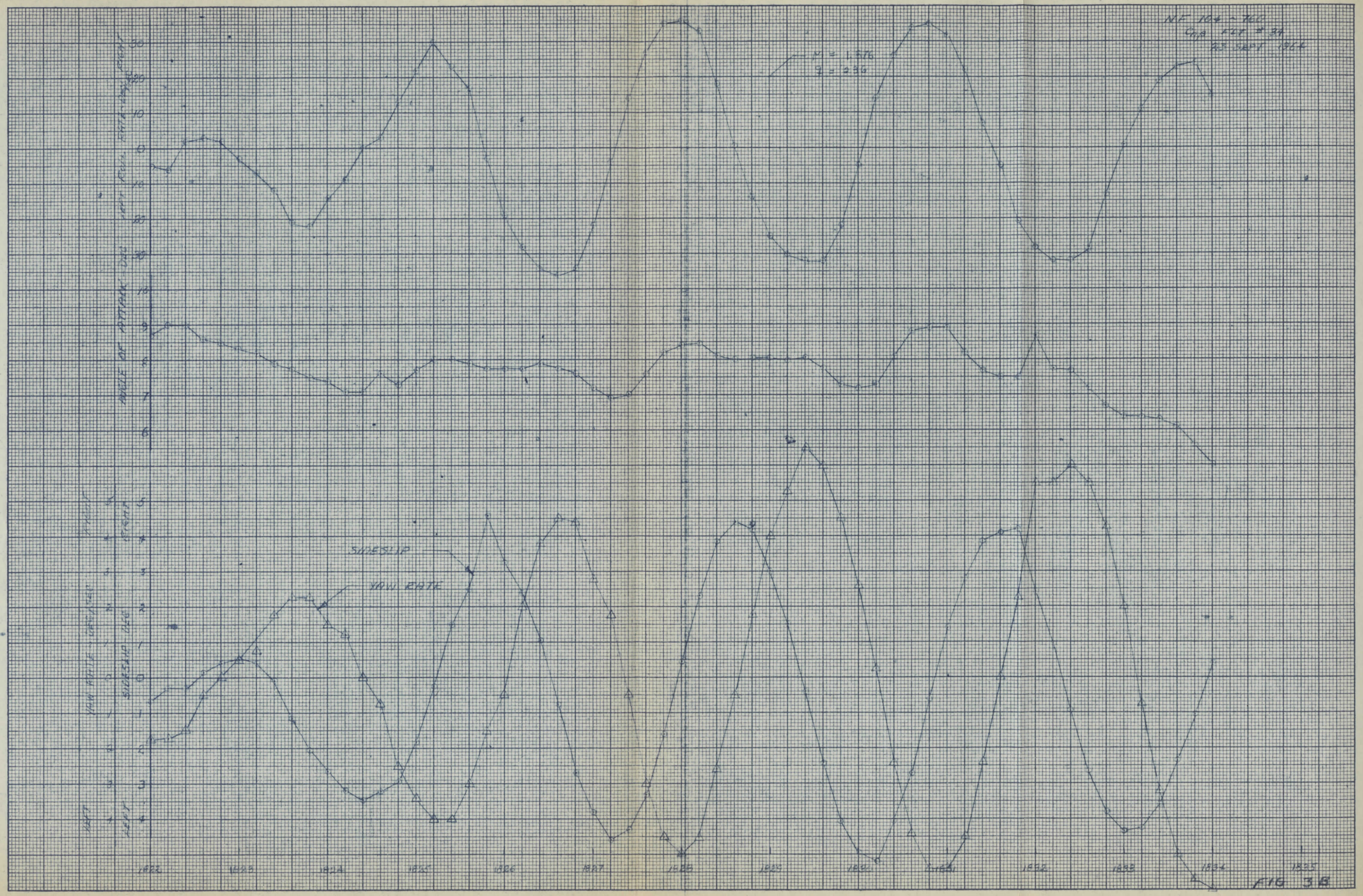

FIG 3B

K&E KEUFFEL & ESSER CO. MADE IN U.S.A. 10 X 10 TO THE CM. 359-1-1472

ANGLE OF ATTACK AND MACH NUMBER FOR C_{m_β} TEST POINTS

DARKENED SYMBOLS INDICATE OSCILLATIONS DIVERGED TO LIMIT CYCLE AMPLITUDE

13 NOV 64

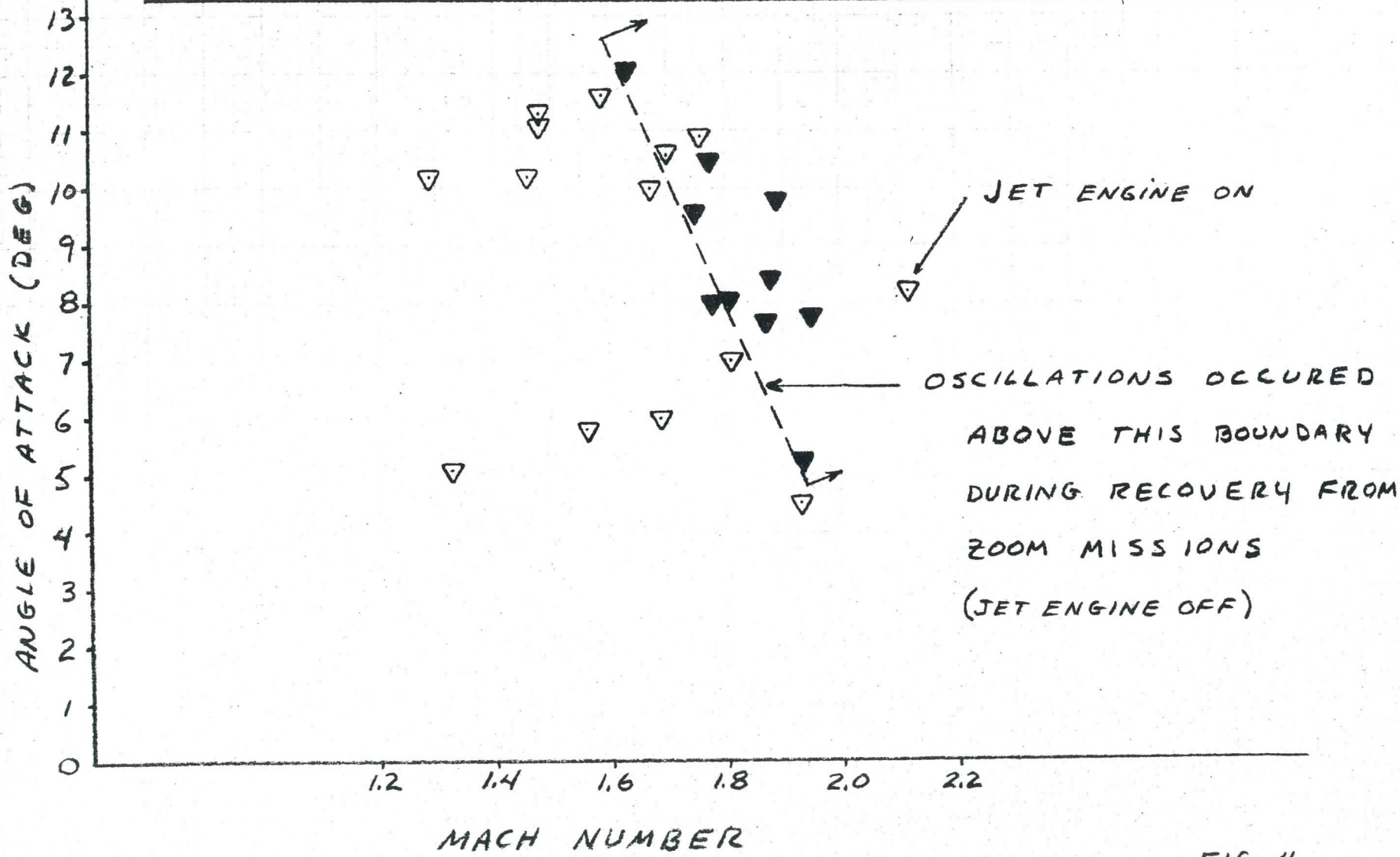

FIG 4

F104 FLIGHT TEST DATA

C_{m_β} vs. MACH NUMBER

STABILITY AXES FLIGHT TEST C.G.

13 Nov 64

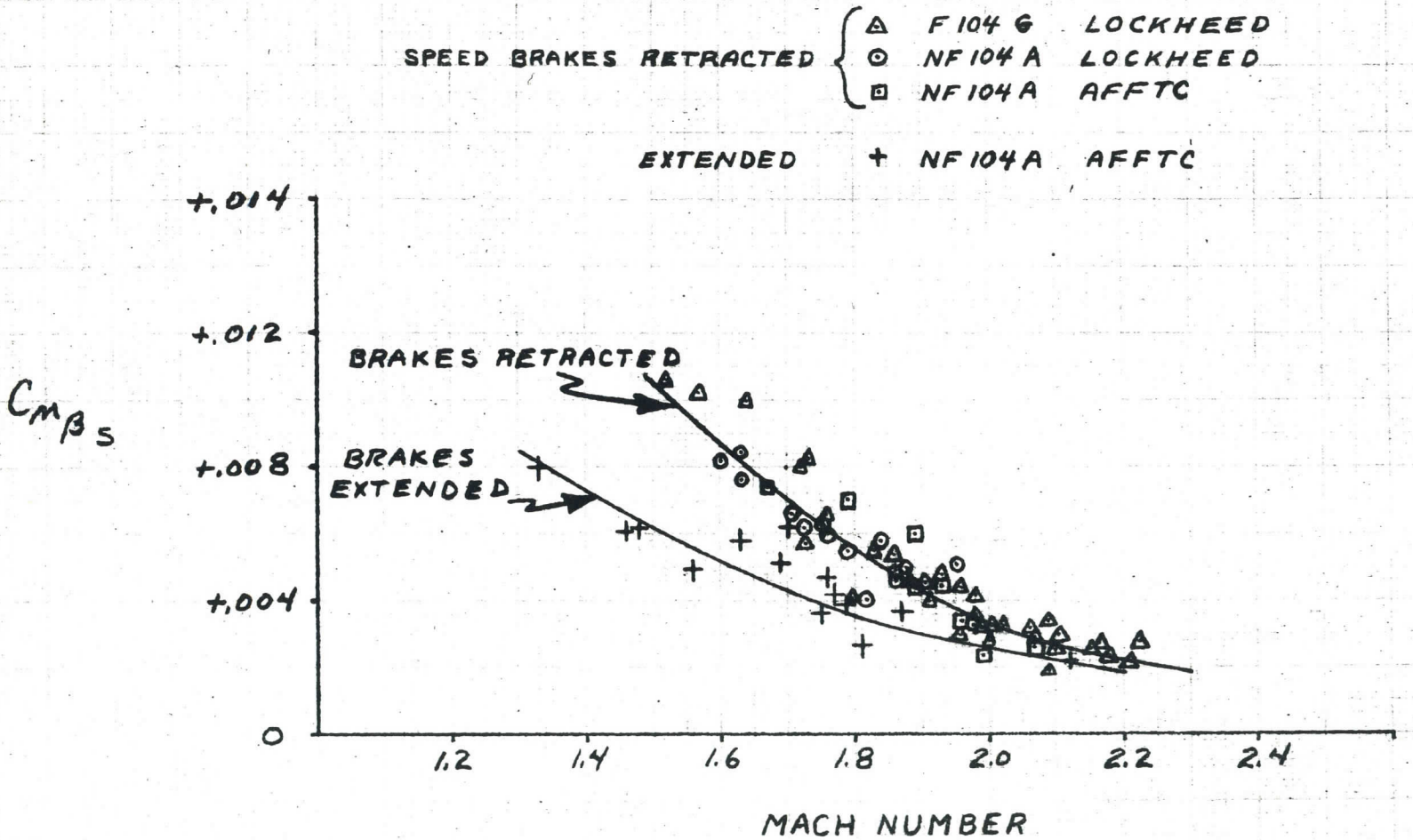

FIG 5

NF 104 FLIGHT TEST DATA

C_{m_β} AND C_{l_β} VS MACH NUMBER

BODY AXES —— FLIGHT TEST C.G.
BRAKES EXTENDED

16 NOV 64

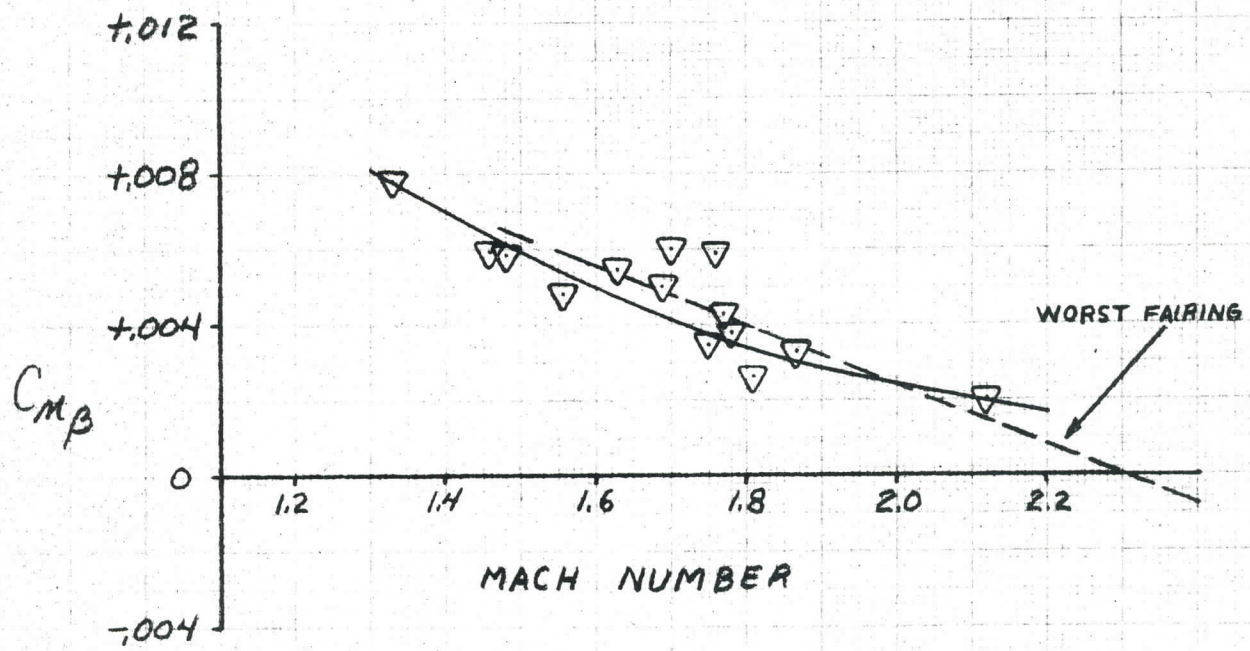

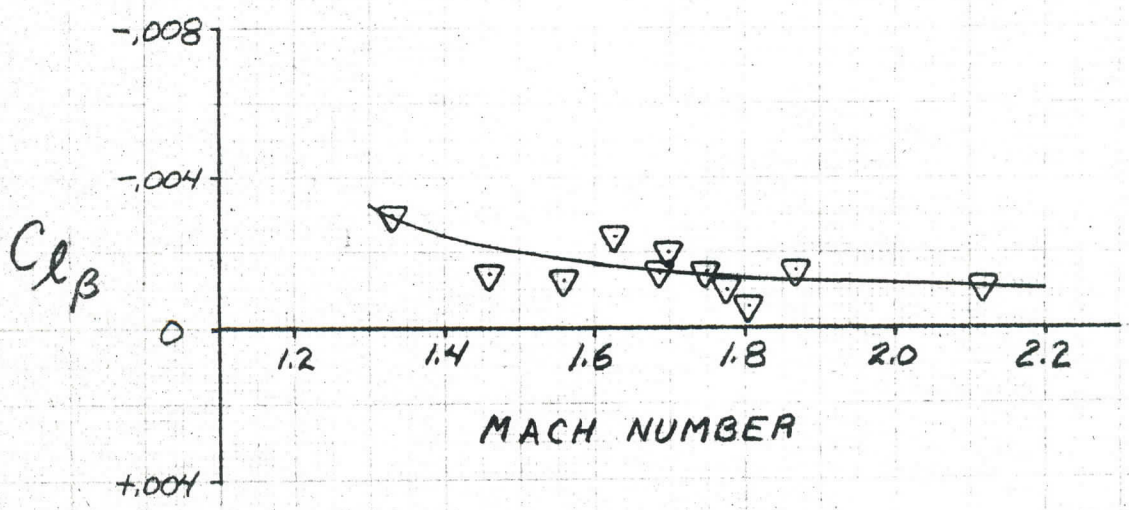

FIG 6

NF 104 FLIGHT TEST DATA

$C_{m\beta}$ vs MACH NUMBER

BODY AXES — CORRECTED C.G.
BRAKES EXTENDED

17 NOV 64

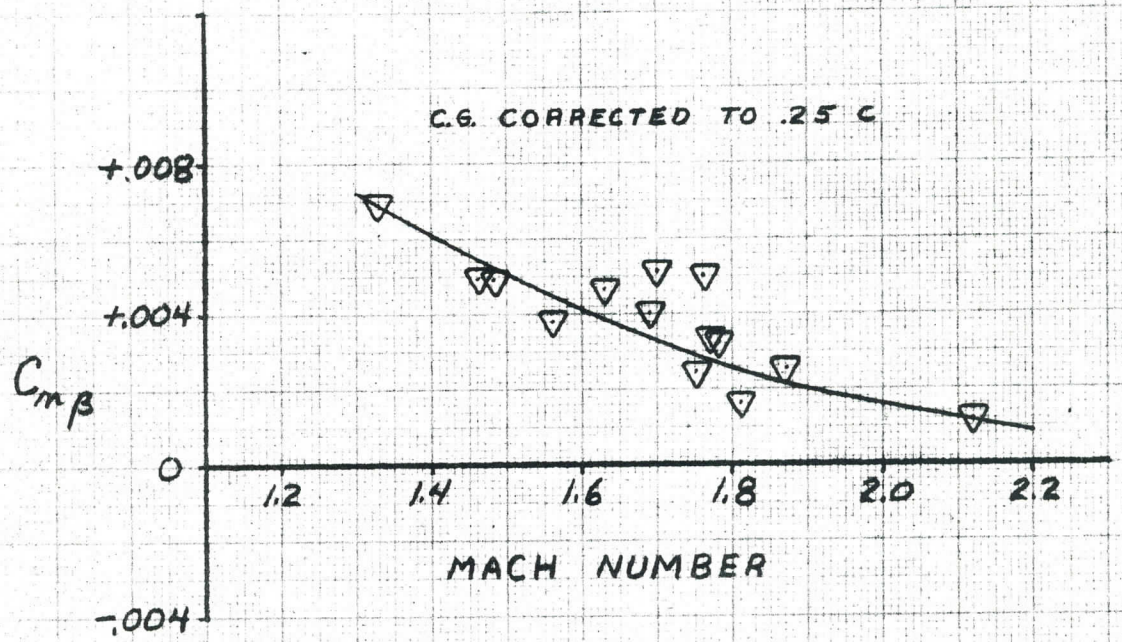

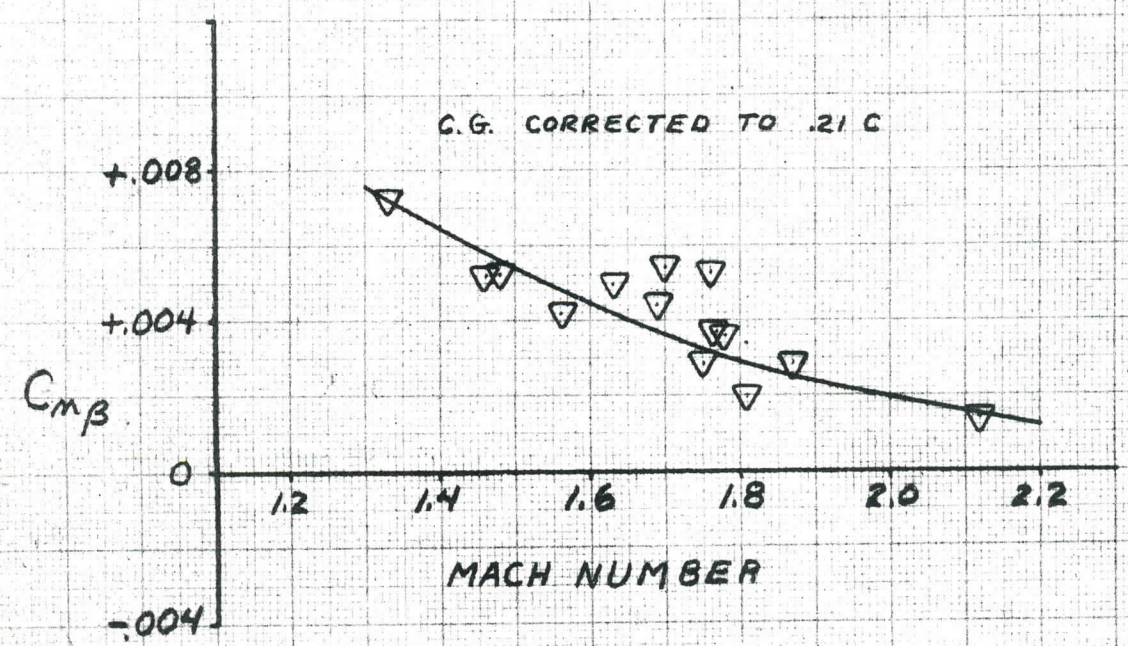

FIG 7

NF104A FLIGHT TEST DATA

C_{m_β} AND C_{l_β} VS. MACH NUMBER

STABILITY AXES – FLIGHT TEST C.G.
BRAKES EXTENDED

16 NOV 64

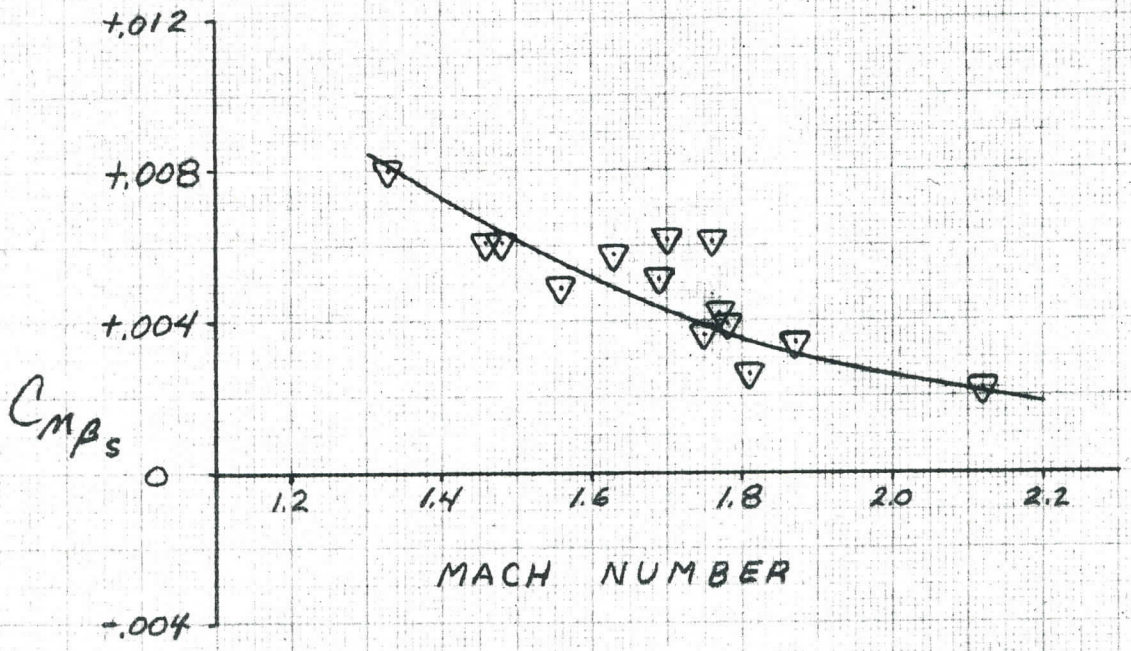

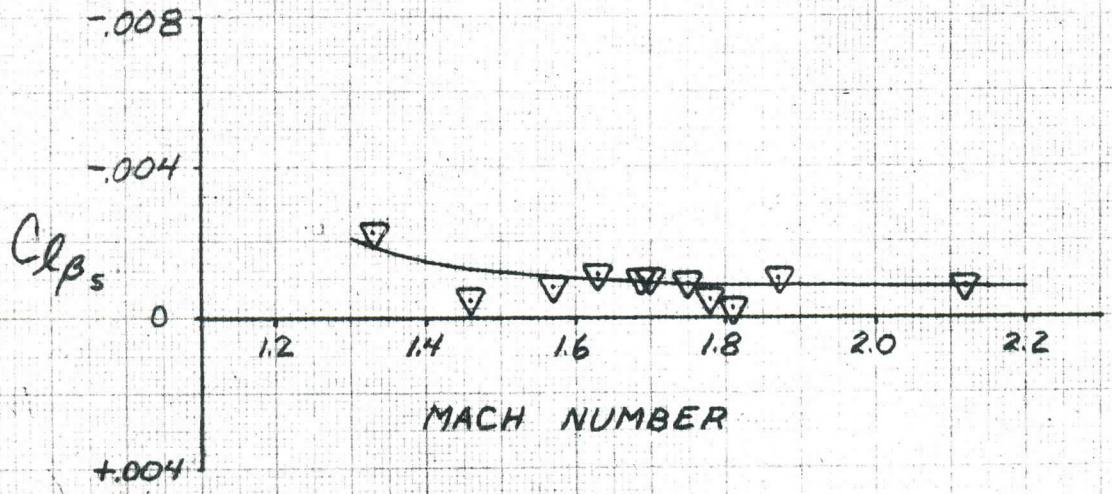

FIG 8

NF 104 FLIGHT TEST DATA

C_{m_β} VS MACH NUMBER

STABILITY AXES — CORRECTED C.G.
BRAKES EXTENDED

17 NOV 64

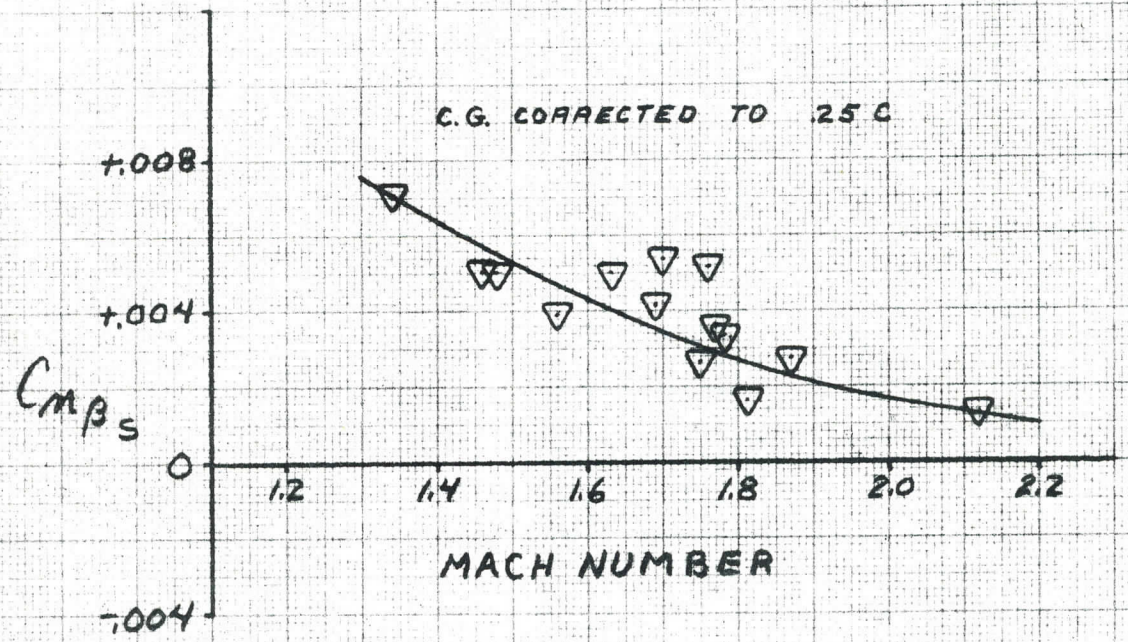

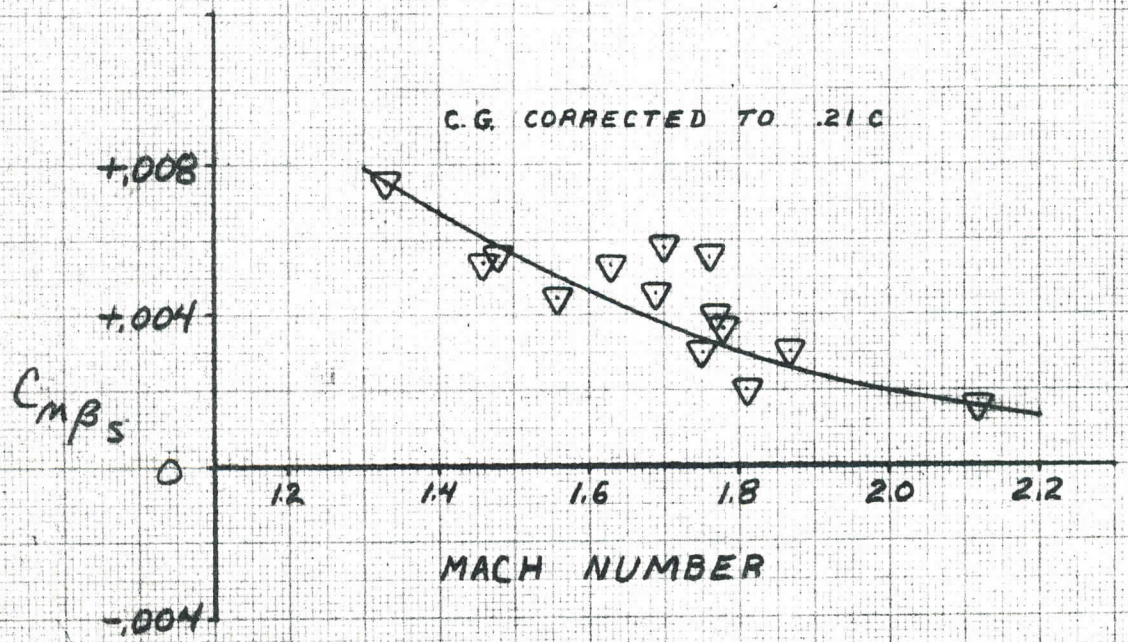

FIG 9

NF 104 A FLIGHT TEST DATA

$C_{m\beta}$ AND $C_{\ell\beta}$ VS MACH NUMBER

STABILITY AXES — FLIGHT TEST C.G.
BRAKES RETRACTED

17 NOV 64

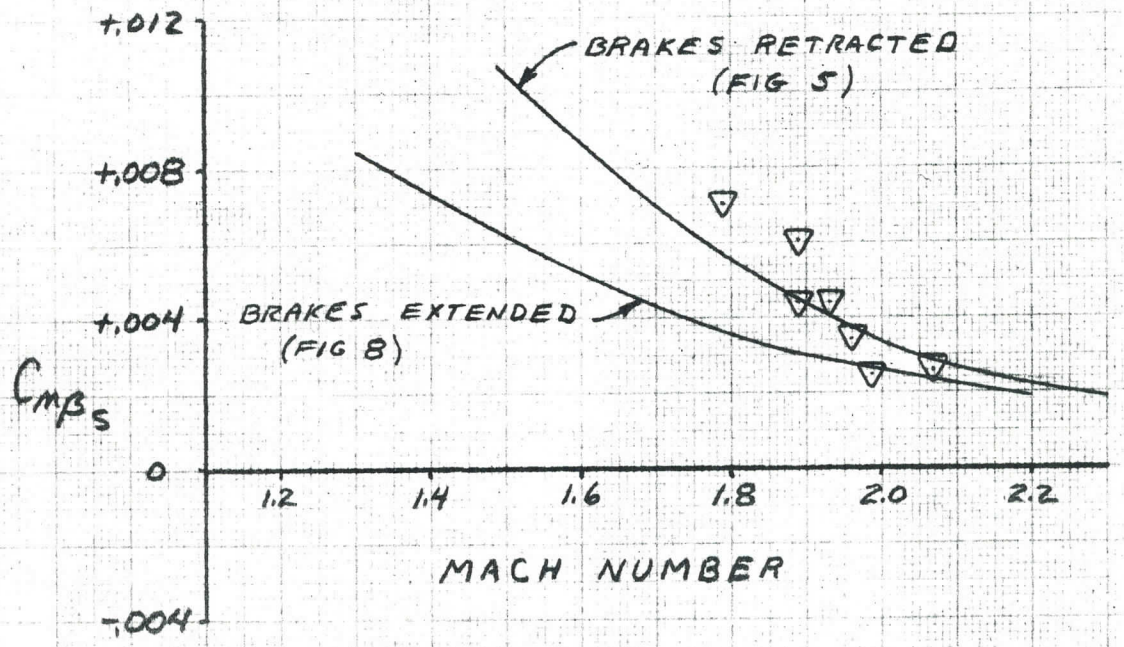

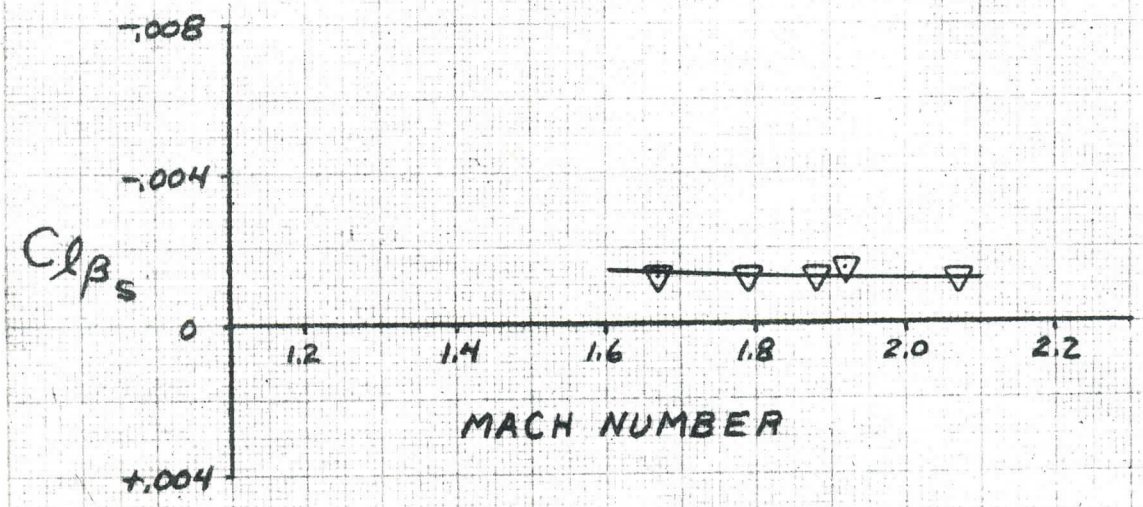

FIG 10

NF 104A LATERAL-DIRECTIONAL DATA
LOCKHEED WIND TUNNEL
STABILITY AXES SPEED BRAKES RETRACTED
13 NOV 64

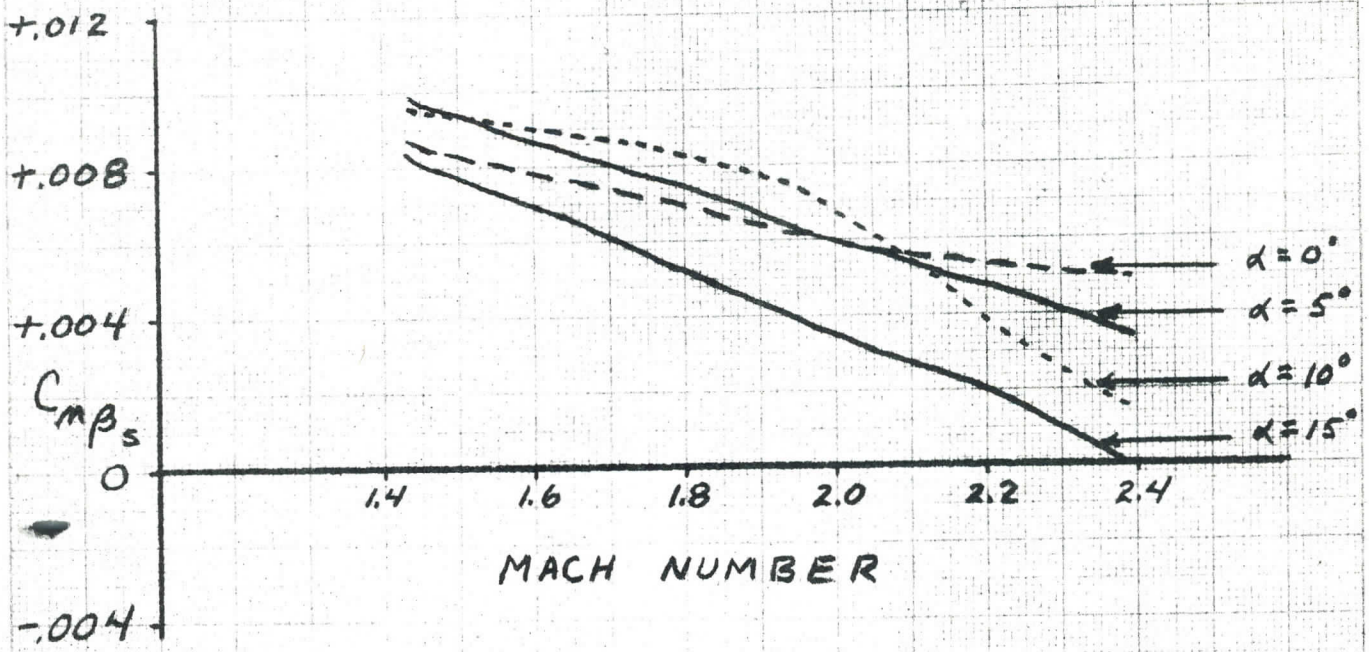

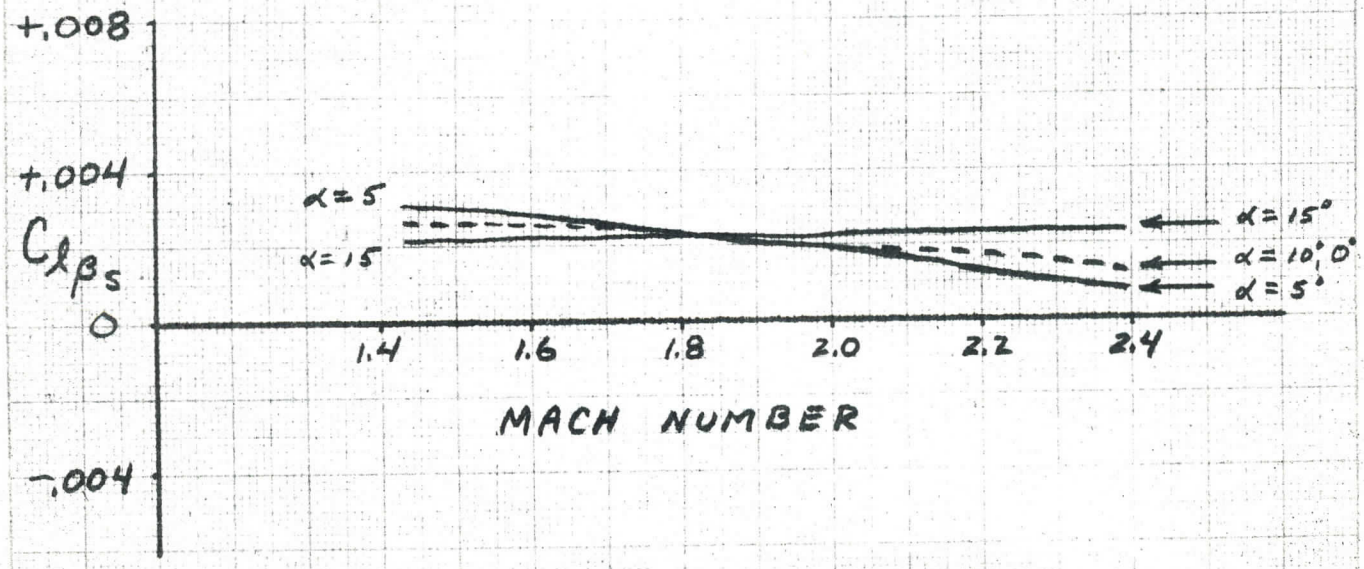

FIG 11